Supplemental data

Cooperative gene activation by AF4 and DOT1L drives *MLL*-rearranged leukemia

Hiroshi Okuda, Boban Stanojevic, Akinori Kanai, Takeshi Kawamura, Satoshi Takahashi, Hirotaka Matsui, Akifumi Takaori-Kondo, Akihiko Yokoyama

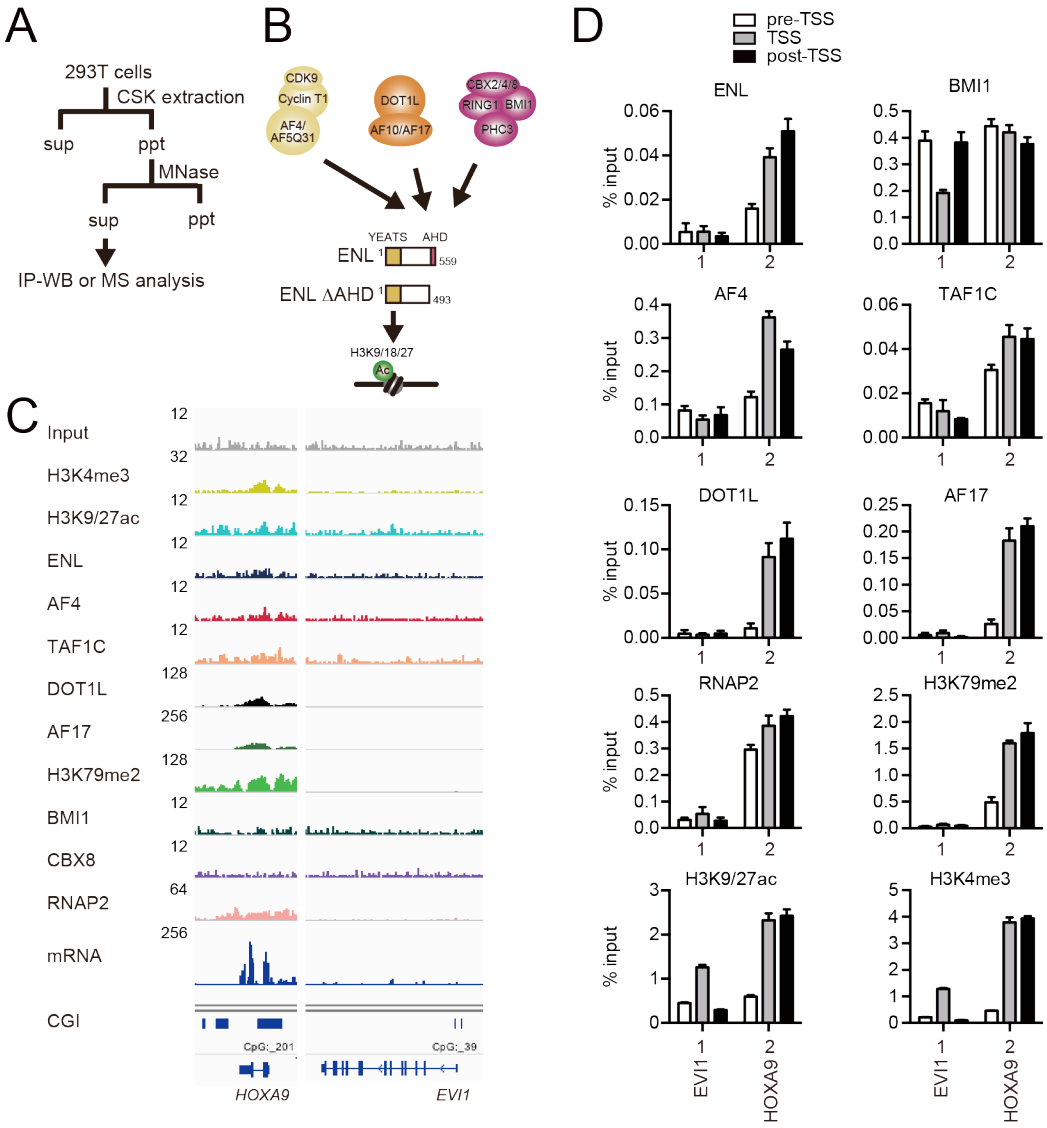

Supplemental Figure 1. AEP co-localizes with DOT1L in the absence of PRC1 in non MLL-rearranged condition

A. nucfrIP analysis. The scheme of the nucfrIP method is shown. CSK: Cytoskelton buffer; MNase: Micrococcal nuclease; sup: supernatant; ppt: pellet.

B. Protein interaction of ENL. ENL associates with three different complexes via AHD.

C. ChIP-seq analysis using 293T cells. The chromatin was analyzed for the HOXA9 and EVI loci by using antibodies specific to indicated proteins/modification, as shown in Figure 1E.

D. ChIP-qPCR analysis using 293T cells. Precipitated DNA was analyzed using specific probes for the pre-TSS (-1.0 to -0.5 kb from the TSS), TSS (0 to +0.5 kb from the TSS), and post-TSS (+1.0 to +1.5 kb from the TSS) regions of the EVI1 and HOXA9 loci. The ChIP signals are expressed as the percent input with error bars (SD of PCR triplicates).

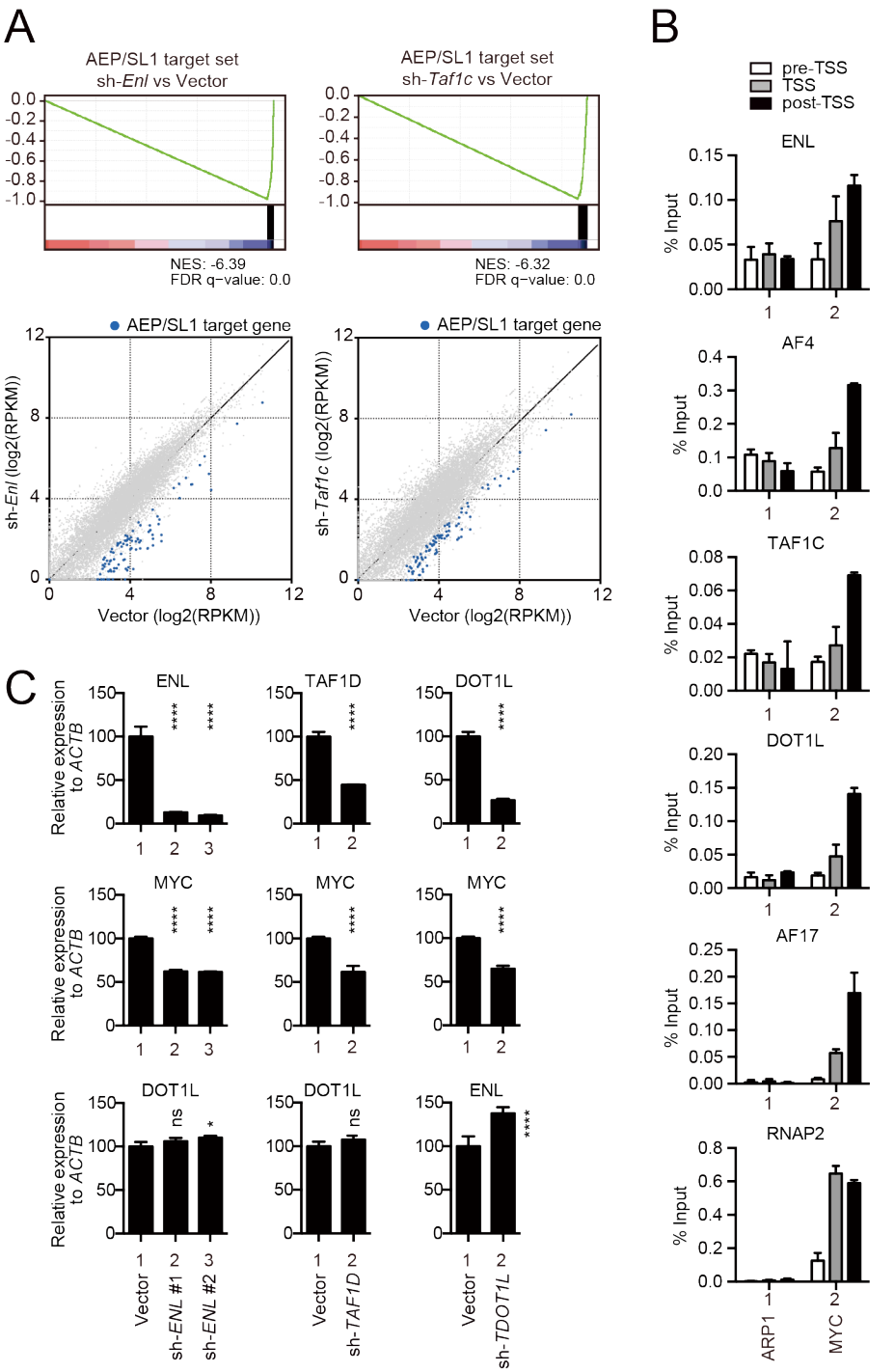

Supplemental Figure 2. Cooperative gene activation by the AEP/SL1 complex and the DOT1L complex in various cell contexts

A. RNA-seq analysis on iMEFs with *Enl* knockdown and *Taf1c* knockdown. GSEA analysis and scatter plot are shown, as in Figure 2B. AEP/SL1 target genes are highlighted in blue. The AEP/SL1 target gene set was defined as the genes whose expression was reduced > 3-fold by shRNAs for both *Enl* and *Taf1c* (1).

B. ChIP-qPCR analysis using K562 cells. Precipitated DNA was analyzed using specific probes for the ARP1 and MYC loci, as shown in Supplemental Figure 1D.

C. *MYC* expression in K562 cells with knockdown of various components of the AEP/SL1 complex or the DOT1L complex. RT-qPCR analysis was performed using K562 cells with or without knockdown of indicated genes. The expression levels normalized to *ACTB* (representative of two independent experiments) are shown relative to the value of the vector control (set at 100%) with error bars (SD of PCR triplicates). Statistical analysis was performed by unpaired t-tests or ordinary one-way ANOVA for each sample compared with the vector control.

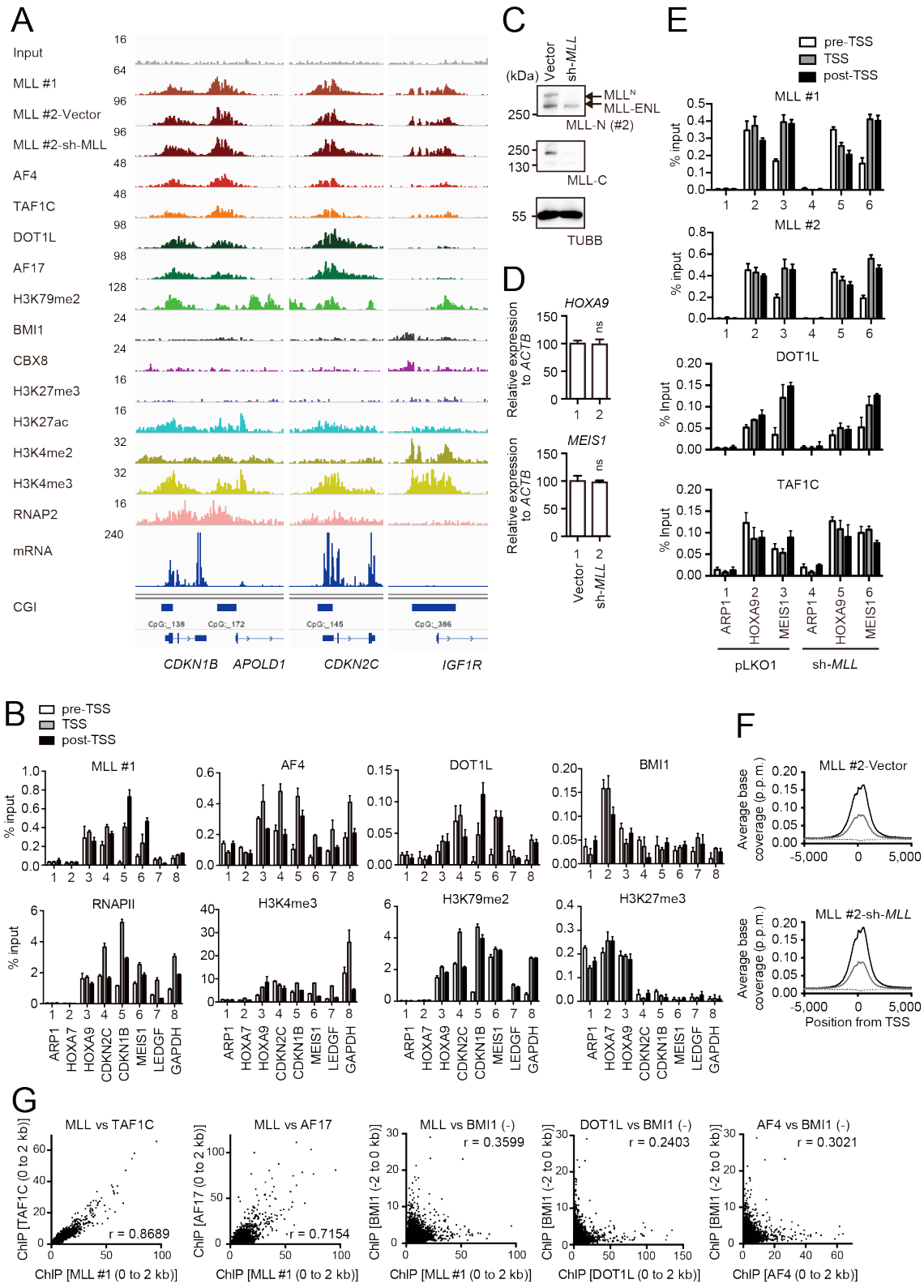

Supplemental Figure 3. Genomic localization of MLL-ENL and various cofactors

A. Genomic localization of various proteins/modifications in HB1119 cells. ChIP-seq analysis was performed, as in Figure 3A.

B. Localization of H3K4me3, H3K79me2, H3K27me3, MLL (Ab#1), AF4, DOT1L, BMI1, CBX8, and RNAP2 at select loci in HB1119 cells. The genomic localization of each protein/modification was determined by ChIP-qPCR, as in Supplemental Figure 1D.

C. Depletion of wt MLL in HB1119 cells. HB1119 cells were transduced with shRNA specific for wt MLL, but not MLL-ENL. Protein expression of MLL-ENL and the MLL^N/MLL^C fragments of wt MLL were analyzed by WB using specific antibodies against MLL. WB for β-tubulin is shown as a loading control.

D. Expression of MLL target genes in wt-MLL-deficient HB1119 cells. RT-qPCR analysis was performed using HB1119 cells with or without knockdown of wt MLL. The expression levels normalized to *ACTB* (representative of two independent experiments) are shown relative to the value of the vector control (set at 100%) with error bars (SD of PCR triplicates). Statistical analysis was performed by unpaired t-tests for each sample compared with the vector control.

E. Localization of MLL proteins and MLL-ENL cofactors with or without knockdown of wt MLL. ChIP-qPCR using two different anti-MLL antibodies and antibodies for DOT1L and TAF1C was performed on select loci, as in Panel B, in HB1119 cells with or without knockdown of wt MLL.

F. Distribution patterns of MLL proteins at the MLL target loci in wt MLL-depleted cells. The distribution pattern of MLL ChIP signal in HB1119 cells with or without knockdown of wt MLL was analyzed, as in Figure 1F.

G. Relative occupations of various factors at MLL target genes. ChIP-seq tags of the MLL target set were analyzed, as shown in Figure 3C.

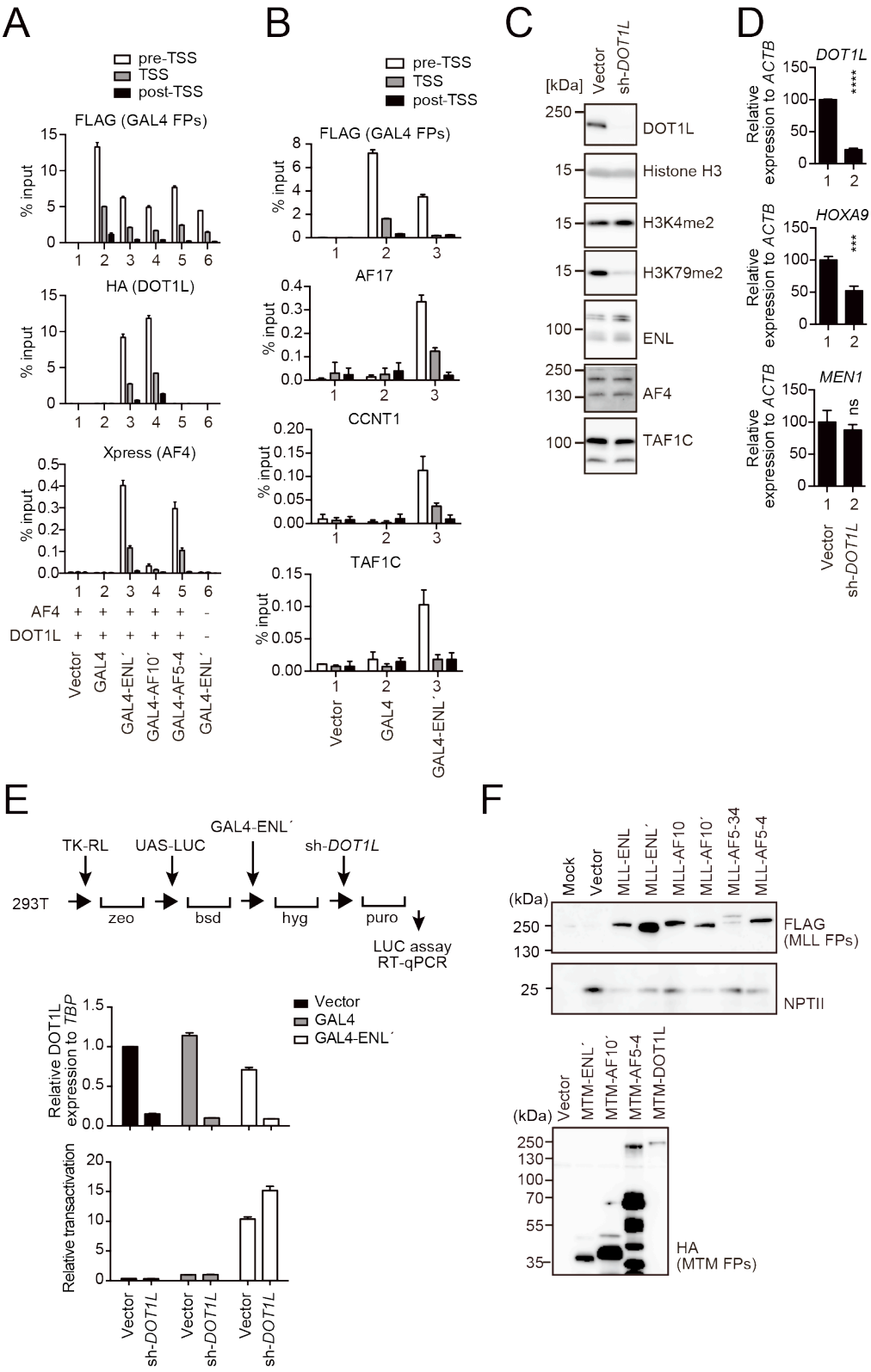

Supplemental Figure 4. Role of DOT1L in AHD-dependent transactivation

A. Co-localization of GAL4 fusion proteins with AF4 and DOT1L on the GAL4-responsive elements. FLAG-tagged GAL4 fusion proteins were transiently expressed with HA-tagged DOT1L and Xpress-tagged AF4 and subjected to ChIP-qPCR with the indicated antibodies. Precipitated DNA was analyzed by qPCR, as in Figure 4C.

B. Co-localization of GAL4-ENL′ with endogenous AEP- and DOT1L complex-components on the GAL4-responsive elements. FLAG-tagged GAL4-ENL′ was analyzed by ChIP-qPCR with the indicated antibodies as in Figure 4C.

C. Protein expression after knockdown of *DOT1L*. 293T cells were transduced with shRNA for *DOT1L* and analyzed by western blot.

D. RT-qPCR analysis after knockdown of *DOT1L* in 293T cells. The expression level normalized to that of *ACTB* (representative of two independent experiments) is shown as the relative value to that of the control vector (arbitrarily set at 100%) with error bars (SD of PCR triplicates). Statistical analysis was performed by unpaired t-tests with the vector control.

E. Transactivation activity of GAL4-ENL′ in the absence of DOT1L. The schema is shown on top. RT-qPCR was performed to confirm DOT1L knockdown. The expression level of *DOT1L* normalized to *TBP* is shown relative to the value of the vector/pLKO.1 control (set at 1) with error bars (SD of PCR triplicates). The promoter activity was assessed using the dual luciferase reporter assay. The transactivation of the GAL4-responsive luciferase reporter gene (UAS-LUC), which was normalized to the Renilla luciferase reporter driven by the promoter of Thymidine kinase (TK-RL), is shown with error bars (SD from triplicates) relative to the value of GAL4/vector (set at 1). A representative result of two independent experiments is shown. zeo: zeocin; bsd: blasticidin ; hyg: hygromycin.

F. Protein expression of the various MLL mutants. The expression of various FLAG-tagged MLL mutants was visualized using an anti-FLAG antibody. The expression level of neomycin phosphatase II (NPTII), which is expressed from the same vector, was also analyzed to confirm comparable transfection efficiency. The expression of HA-tagged MTM mutants in the virus packaging cells was visualized using an anti-HA antibody.

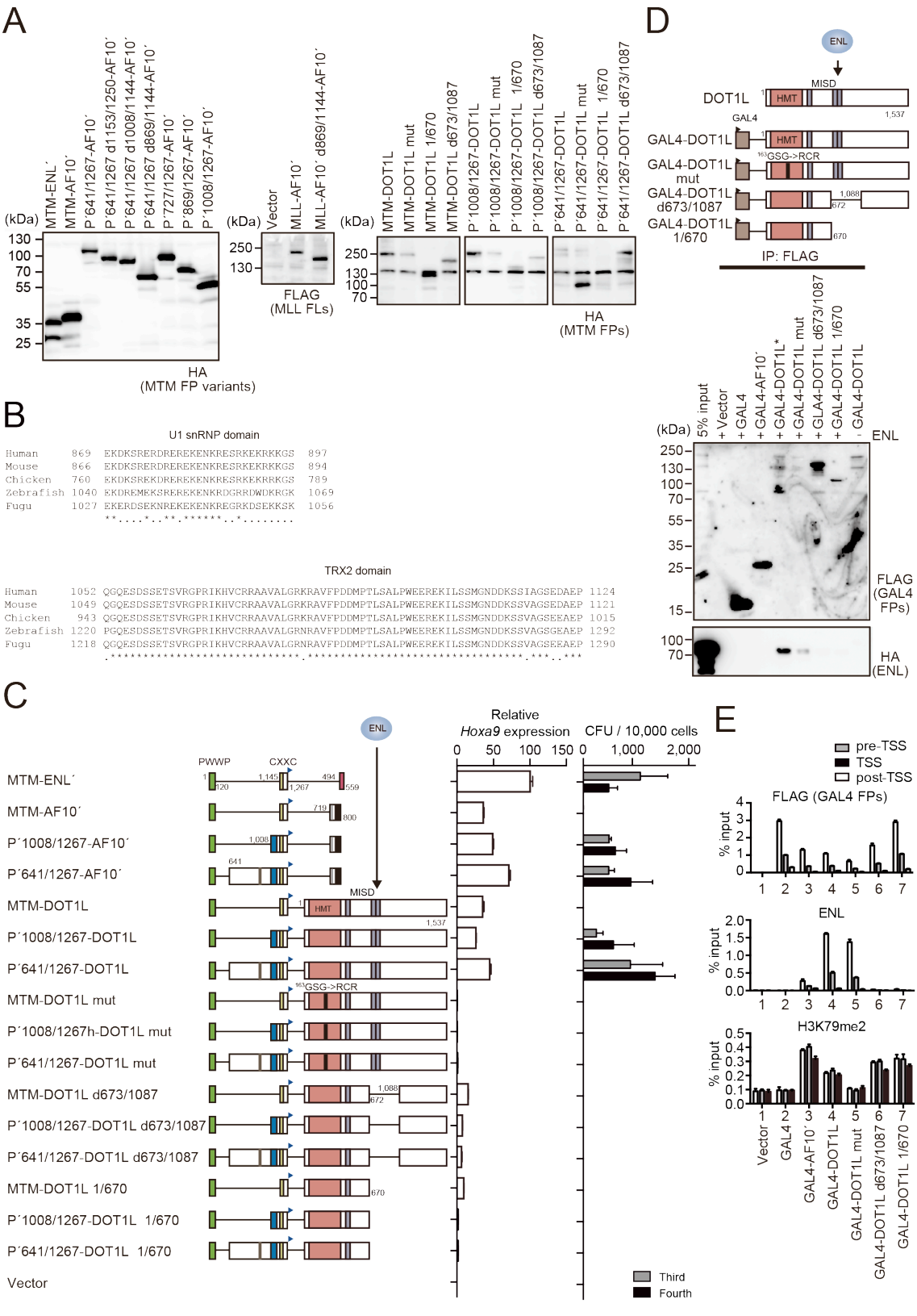

Supplemental Figure 5. Structural requirement for MLL-DOT1L-dependent transformation

A. Protein expression of the various MLL mutants. The expressions of various FLAG-tagged MLL mutants and HA-tagged MTM mutants in the virus packaging cells were visualized using anti-FLAG and HA antibodies, respectively.

B. Sequence similarity of the U1 snRNP domain and the TRX2 domain among species. Sequence alignment of various MLL orthologs is shown.

C. Transforming potential of various MLL-DOT1L mutants. Various constructs were analyzed, as in Figure 5A.

D. Association of ENL with various GAL4-DOT1L/AF10 mutant proteins. GAL4- DOT1L/AF10 fusion proteins were analyzed by fanChIP-WB using anti-FLAG antibody, as in Figure 4B. The co-precipitated proteins were visualized using specific antibodies for the indicated tags.

E. ENL recruitment and H3K79 methylation by various GAL4-DOT1L fusion proteins. GAL4-DOT1L/AF10 fusion proteins were analyzed by ChIP-qPCR, as in Figure 4C. faxChIP was employed for the ChIP analysis of H3K79me2.

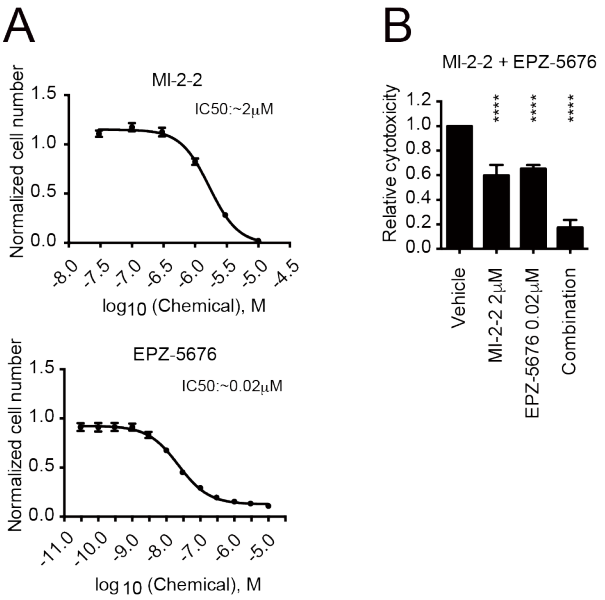

Supplemental Figure 6. The combinatorial effect of the MENIN-MLL interaction inhibitor and the DOT1L HMT inhibitor on a human MLL-AF4 leukemia cell line

A. Sensitivity of MV4-11 cells to MI-2-2 and EPZ-5676. MV4-11 cells carry the t(4;11) translocation and express MLL-AF4 and AF4-MLL fusion proteins endogenously. Cell viability was measured on Day 5. The experiment was repeated four times independently in tetraplicate.

B. Combined effects of the simultaneous use of MENIN-MLL inhibitor (MI-2-2) and DOT1L inhibitor (EPZ-5676) on MV4-11 cells. Statistical analysis was performed by ordinary one-way ANOVA comparing with the vehicle control

Supplemental Table 1. Antibodies used in this study

Antigen	Antibody type	ID/product no.	Source/reference	Application
FLAG tag	Rabbit polyclonal	F-7425	Sigma	WB
FLAG tag	Mouse monoclonal	F-3165	Sigma	WB, ChIP
HA tag	Rat monoclonal	3F10	Roche	WB, ChIP
Xpress tag	Rabbit polyclonal	sc-499	Santa Cruz Biotech.	WB
Xpress tag	Mouse monoclonal	sc-7270	Santa Cruz Biotech.	IP, ChIP
AF4	Goat polyclonal	sc-49350	Santa Cruz Biotech.	WB, ChIP
AF5Q31	Rabbit polyclonal	A301-538A	Bethyl Laboratories	WB
AF17	Rabbit polyclonal	A302-198A	Bethyl Laboratories	WB, ChIP
BMI1	Rabbit monoclonal	6964	Cell Signaling	WB, ChIP
CBX2	Rabbit polyclonal	A302-524A	Bethyl Laboratories	WB
CBX8	Rabbit polyclonal	61238	Active Motif	ChIP
Cyclin T1	Rabbit polyclonal	A303-497A	Bethyl Laboratories	WB
Cyclin T1	Goat polyclonal	sc-8127	Santa Cruz Biotech.	ChIP
DOT1L	Mouse monoclonal	sc-390879	Santa Cruz Biotech.	WB
DOT1L	Rabbit polyclonal	A300-953A	Bethyl Laboratories	ChIP
ENL	Rabbit polyclonal	A302-267A	Bethyl Laboratories	WB, ChIP
Histone H3	Rabbit polyclonal	39163	Active Motif	WB
H3K4me2	Rabbit polyclonal	ab7766	abcam	WB
H3K4me3	Rabbit polyclonal	39159	Active Motif	ChIP
H3K9/27ac	Rabbit polyclonal	305-34853	MAB Institute Inc. *1	ChIP
H3K27ac	Rabbit polyclonal	ab4729	abcam	ChIP
H3K27me3	Mouse monoclonal	301-95253	MAB Institute Inc. *1	ChIP
H3K79me2	Rabbit polyclonal	ab3594	abcam	WB, ChIP
MENIN	Rabbit polyclonal	A300-105A	Bethyl Laboratories	ChIP
MLL^N	Rabbit polyclonal	rpN1	(2)	ChIP
MLL^N	Rabbit monoclonal	14689	Cell Signaling	WB, ChIP
MLL^C	Rabbit monoclonal	14197	Cell Signaling	WB,
NPT II	Rabbit polyclonal	06-747	Millipore	WB
RNAP2	Mouse monoclonal	05-263	Millipore	ChIP

TAF1C	Rabbit polyclonal	A303-698A	Bethyl Laboratories	WB, ChIP
TUBB	Rabbit polyclonal	ab6046	abcam	WB

*1 The initial batch was a generous gift from Dr. Hiroshi Kimura, Tokyo Institute of Technology, Yokohama

Supplemental Table 2. Primers used in this study

	Forward primer seq.	Reverse primer seq.	Reporter seq.
ARP1 pre-TSS	AGGGCAGTTGCTCTGAAGTC	CTGCAGAAGGAGCTCTTGGA	ACTGCCTGGCCACTCC
ARP1 TSS	AGAGAGAGTGCGAGACCGA	GCCACTGGCAGTTTCTTTCTG	CCTCTCCAGCTTTCTC
ARP1 post-TSS	CAGGCCCAAGCGAATTACCT	AGTTGACTGGTGATCAATTTAAAGGAGTT	CTGGATGCCAAGCTCT
EVI1 pre-TSS	TCACCAGACAGTCATCAATCTCTCT	GAAGGGCGTGCAAAATTTTCAAAC	CCCGCCCAAACAGCAT
EVI1 TSS	GCTGCGGAGGATCTGAAAGG	CTCCTTCCCAGTTCCAATGGG	CAGGAGGAGGAGAGTTT
EVI1 post-TSS	CACCACCCTTCATCTCTTTAGCAT	TGGCAGCTTCCTGGAGATATAAAAG	AAGCTGAGATTTTCCC
HOXA7 pre-TSS	GCCTTCCCCGTCTGGAT	ACTCTGCCCAAGTCTTCTCTCA	CAGGCCGGACTTAGAC
HOXA7 TSS	GACGCCTACGGCAACCT	GCCTTTGGCGAGGTCACT	CCCTGCGCCTCCTAC
HOXA7 post-TSS	TGCCAGGGTCCATTTCAAGATG	CCCTCATCCCCAGGACCTT	CTCTGTCCTCATTCCC
HOXA9 pre-TSS	TGGCTGCTTTTTTATGGCTTCAATT	CCGCGTGCGAGTGC	CCCCTCACATAAAATT
HOXA9 TSS	TCACCACCACCCCTACGT	GCAAGCCCGCGAAGGA	CAGGAGCGCATGTACC
HOXA9 post-TSS	AGTGGCGGCGTAAATCCT	TGATCACGTCTGTGGCTTATTTGAA	CCCGCAGCCTCATC
CDKN1B pre-TSS	GTCCCGAGGGTCCCTTC	GTGTGCCTACCTCATCTCATACG	CAGCTGTCACATTCTG
CDKN1B TSS	GGGTCTGTGTCTTTTGGCT	GCCCGAACCCCTCTCG	CCAGCGACTGCCCTC

CDKN1B post-TSS	GCTTTGGGAGAGCTAACTTTATTGGT	CGGATCTTACCATCTCCAGTTTCTG	ACCTGGCCCACTGCTT
CDKN2C pre-TSS	CTCCACAACCGTCTTAAATAACAAACC	GCGGGCTTGAGTCTGTGA	CAGCTGCCCCAATTC
CDKN2C TSS	GGCGGCTGCCCTGT	CCCGGTGCCACTTTGC	CTGTGCCCCTTTGCTG
CDKN2C post-TSS	CTGTGGAGTCGTCAGAATTCTTTCAT	CGATTCACACGTGATTATTCAGCAAA	CCTCGCCTCGCTTTT
LEDGF pre-TSS	CCACCTACCAGCTCCTATTCTACTA	GGATGTGAGTTTGGGCCCTAA	TAGCTGCATCTAAATTTT
LEDGF TSS	CCCCGGCAGGTGAGC	GCCCAGCGGCTGCA	TTCCCCGCTACAGCCAG
LEDGF post-TSS	TGTTTAAAAATTAGTGAAACATTGACATTTCCATAGTT	TTCTCTGACATCCAAGTGTTTGTGT	TTGGATCAAGTACAAAATATC
MEIS1 pre-TSS	CGGCGTTGATTCCCAATTTATTTCA	CACACAAACGCAGGCAGTAG	CCGCCAGCTTTATTTT
MEIS1 TSS	TTTGCTTCAGGTCCCGTAGAC	CCTTAACGTCTCCAGCAACGT	ACTGGTCCCAGATCTT
MEIS1 post-TSS	TCTCAGCGCCTCCAAATCTTG	TTTGTGTGTGTGAAATTTAGCTATTTAGGTTTT	CCAGGCAGTTATTTTC
MYC pre-TSS	GCGGTATCTGCTGCTTTGG	GCATTATGTATGCACAGCTATCTGGAT	CTGGGTGGAAGGTATCC
MYC TSS	CCGGCTAGGGTGGAAGAG	GAGGCGAAGCCCCCTATTC	CAGGACGCCCGCAGCG
MYC post-TSS	GGGTAGGCGCAGGCA	GGTTTTTCCAAGTCAACGATTCCA	ATGTGTCCGATTCTCC
GAPDH pre-TSS	CCCCTCCTAGGCCTTTGC	GCTGAGAGGCGGGAAAGTT	ACTACCGCAGAGCCTC
GAPDH TSS	CCACATCGCTCAGACACCAT	GCGAACTCACCCGTTGACT	CCGACCTTCACCTTCC

GAPDH post-TSS	GGCTCTCTCCCATCCCTTCT	AGGAGTGGGAGCACAGGTAA	CCCCACACACATGCAC
LUC pre-TSS	CGGCGCCATTCTATCCTCTAG	AGGGCGTATCTCTTCATAGCCTTAT	CTCCAGCGGTTCCATC
LUC TSS	GGGCTGAATACAAATCACAGAATCG	CCAACACCGGCATAAAGAATTGAAG	ATGCAGTGAAAACTCT
LUC post-TSS	CATCACGGTTTTGGAATGTTTACTACA	GGGATCGTAAAAACAGCTCTTCTTCA	ACGACTCGAAATCCAC

Supplemental Table 3. Primers used for RT-qPCR in this study

TaqMan Probes for mouse transcripts

Gene	Probe ID
Gapdh	Mm99999915_g1
Actb	Mm00607939_s1
Dot1l	Mm01171419_g1
Tbp	Mm00446971_m1
Taf1c	Mm00498790_m1
Enl (Mllt1)	Mm00452080_m1
Mll (Mll1)	Mm01179235_m1
Hoxa9	Mm00439364_m1
Hoxc8	Mm00439369_m1
Hoxc9	Mm00433972_m1
Cdkn2c	Mm00483243_m1

TaqMan Probes for human transcripts

Gene	Probe ID
ACTB	Hs99999903_m1
TBP	Hs00427620_m1
DOT1L	Hs01588547_m1
HOXA9	Hs00365956_m1

MEN1	Hs00365720_m1
ENL	Hs00172962_m1
TAF1D	Hs00225533_m1
MYC	Hs01570247_m1

References

1. Okuda H, Kanai A, Ito S, Matsui H, and Yokoyama A. AF4 uses the SL1 components of RNAP1 machinery to initiate MLL fusion- and AEP-dependent transcription. *Nat Commun*. 2015;6(8869.
2. Yokoyama A, Kitabayashi I, Ayton PM, Cleary ML, and Ohki M. Leukemia proto-oncoprotein MLL is proteolytically processed into 2 fragments with opposite transcriptional properties. *Blood*. 2002;100(10):3710-8.